ELSEVIER

Biochimica et Biophysica Acta 1363 (1998) 147–156

BIOCHIMICA ET BIOPHYSICA ACTA
BBA

Non-photochemical quenching of chlorophyll fluorescence in photosynthesis. 5-hydroxy-1,4-naphthoquinone in spinach thylakoids as a model for antenna based quenching mechanisms

Sergej Vasil'ev, Scott Wiebe, Doug Bruce *

Department of Biological Sciences, Brock University, St. Catharines, ON, Canada L2S 3A1

Received 7 July 1997; accepted 6 November 1997

Abstract

In vivo mechanisms of non-photochemical quenching that contribute to energy dissipation in higher plants are still a source of some controversy. In the present study we used an exogenous oxidized quinone, 5-hydroxy-1,4-naphthoquinone to induce quenching of chlorophyll excited states in photosynthetic light-harvesting antenna and to elucidate the mechanism of non-photochemical quenching of chlorophyll fluorescence by this quinone. Excitation dynamics in isolated spinach thylakoids in the presence of an exogenous fluorescence quencher was studied by a combined analysis of data gathered from independent techniques (fluorescence yields, effective absorption cross-sections and picosecond kinetics). The application of a kinetic model for photosystem II to a combined data set of fluorescence decay kinetics and absorbance cross-section measurements was used to quantify antenna quenching by a model antenna quencher, 5-hydroxy-1,4-naphthoquinone. We observed depressions in F_0 and photosystem II absorption cross-sections, paralleled with an increase of the rate constant for excitation decay in antenna. This approach is a first step towards quantifying the amount of antenna quenching contributing to non-photochemical quenching in vivo, evaluation of the contributions of antenna and reaction centre mechanisms to it and localization of the sites of non-photochemical energy dissipation in intact plant systems. © 1998 Elsevier Science B.V.

Keywords: Chlorophyll fluorescence quenching; Quinone; Thylakoid membrane; Absorption cross-section; Time-resolved fluorescence

1. Introduction

Processes of non-photochemical quenching (qN) serve a protective role against the light induced inhibition of photosynthesis. Inhibition of photosynthetic capacity can arise because the absorption of energy in the physiological range of light intensity may be much higher than photochemical utilization of that energy. The resulting surplus of energy becomes a potential source of damage to the plant, as it can lead to formation of destructive oxidative molecules such as singlet oxygen radicals. Oxidative molecules can damage the photosynthetic apparatus in a process called photoinhibition [1,2]. In order to avoid photoinhibition, nature provided plants with a fine-tuned mechanism to regulate the dissipation of excess en-

Abbreviations: qN: non-photochemical quenching; qE: energy-dependent quenching; qT: state transitions; 5-OH-NQ: 5-hydroxy-1,4-naphthoquinone; FWHM: full width at half maximum; DAS: decay-associated spectrum; PQ: plastoquinone; Chl z: alternative electron donor for photosystem II; Chl: chlorophyll

* Corresponding author. Fax: +1-905-688-1855; E-mail: dbruce@spartan.ac.brocku.ca

PII S0005-2728(97)00096-0

ergy. These processes (non-photochemical quenching, qN) promote the dissipation of energy through 'safe' heat loss pathways and consequently decrease chlorophyll a fluorescence yield [3]. There are two reversible components to qN: the state transitions, qT and energy-dependent quenching, qE (see Refs. [2,4–7] for the reviews). qE is thought to be the largest component of qN. It is regulated by the pH gradient across the thylakoid membrane [8,9] and may involve either an antenna complex mechanism that decreases the efficiency of energy transfer to the reaction centre [10] or an alternative electron transfer pathway in the reaction centre. Mechanisms proposed for antenna quenching include quenching by carotenoids of the xanthophyll cycle [11–14] and/or aggregation of antenna chlorophyll–protein complexes [15–18]. Charge recombination, cyclic electron transport and quenching by oxidized P680 and/or Chl z have been proposed to account for reaction centre quenching [19–22].

What is the mechanism and location of qE in vivo? Are there contributions from both antenna and reaction centre mechanisms? Various techniques in fluorescence spectroscopy have been used to approach these questions. However, due to the complexity of the system few studies attempt to give quantitative answers based on current kinetic models of the excited state dynamics of PSII. The use of simplified model systems which mimic either antenna or reaction centre based mechanisms of qE is an approach which may allow kinetic modeling of qE process.

One model antenna quenching system involves the addition of quenching molecules which compete with excitation energy transfer. It is well established that exogenous oxidized quinones quench Chl fluorescence. Substituted quinones are known to interact with excited chlorophyll molecules in solution and quench excitation via a mechanism that involves transient charge separation between Chl and quinone [23,24]. Two mechanisms have been suggested to account for quenching of Chl fluorescence in vivo: Some groups suggest that certain quinones interact with the D-1 polypeptide, compete with Q_B for its binding site, and steal the excess energy at the level of electron transport [25–28]; others have shown that quinones interact directly with excited chlorophyll molecules in the antenna [23,29,30].

The main focus of this research was to study excitation dynamics in intact PSII in the presence of an exogenous fluorescence quencher by a combined analysis of data gathered from independent techniques (fluorescence yields, effective absorption cross-sections and picosecond kinetics). Could the data sets arising from treatments with various concentrations of 5-OH-NQ be evaluated with a global kinetic model assuming pure antenna quenching? The present study indicates that 5-OH-NQ quenches fluorescence in the antenna with well-defined effects on steady-state fluorescence yields, absorption cross-sections, and picosecond decay kinetics. We plan to relate these results to future studies of non-photochemical quenching in vivo. The responses defined here will act as diagnostics for antenna quenching mechanisms, complementary to responses previously investigated in an artificially-quenched reaction centre [21].

2. Materials and methods

Thylakoids were isolated from market spinach as described in Whitmarsh and Ort [31] and stored at -80°C at a concentration of about 2 mg Chl ml^{-1}. For measurements the thylakoids were diluted in buffer (0.2 M sorbitol, 5 mM Hepes, 2 mM $MgCl_2$, 0.5 g l^{-1} BSA, pH 7.5) to a final concentration of 10 μg Chl ml^{-1}. Chlorophyll concentrations were measured according to Zeigler and Egle [32].

PSII absorption cross-sections were determined by recording flash saturation curves of Chl a fluorescence yield as outlined by Samson and Bruce [33]. Non-actinic pulses of light were supplied by a low intensity xenon flash lamp covered with a short-pass blue filter. Actinic laser pulses (250 ns FWHM) were generated by a Phase-R DL-32 dye laser operating at 650 nm. The time between actinic and probe flashes was 70 μs. A small fraction of the laser flash was directed to a pyranometer (Molectron) to measure the energy of actinic pulses. Each data point of the fluorescence saturation curve is an average of 8 fluorescence yield and actinic excitation signals collected at a flash frequency of about 0.15 Hz. Data curves were fit with the cumulative Poisson single-hit probability distribution as described in [34]: $F(I) = F_0 + F_v\ (1 - e^{-I\cdot\sigma})$ where I is the flash intensity (photons/Å^2), $F(I)$ is the yield of photoproduct

measured (fluorescence), F_0 is the minimum yield of fluorescence (no pump flash), F_v is the maximum yield of variable fluorescence (F_{sat}–F_0) where F_{sat} is the maximum yield of fluorescence induced by a saturating single turnover pump flash, and σ is the effective absorption cross-section (Å^2).

Fluorescence decay kinetics were measured with the single photon counting apparatus described previously [21]. The sample was excited at 665 nm by laser pulses with FWHM of about 60 ps delivered by a Hamamatsu picosecond diode laser PLP-01 set to 10 MHz repetition rate. Part of the excitation pulse reflected from a glass plate was focused onto a fast avalanche photodiode used as the timing reference. Fluorescence emission was detected by a Hamamatsu R-2809 MCP screened by a double monochromator. This yielded an instrument response function of about 70 ps. Instrument response functions were collected as background decay from cold, circulating water at 665 nm. Fluorescence decays were recorded between 680 and 700 nm (interval 5 nm) with 30 000 counts in the peak channel. The samples (0.5 l, 10 μg Chl ml^{-1}) were kept in the dark and pumped with a flow speed of about 400 ml min^{-1} through a laboratory built nozzle forming a 1 mm diameter jet used as the measurement area for detection of fluorescence. This allowed the preparation to remain at F_0 with open reaction centers. All samples were kept on an ice bath during measurement to avoid destabilization of the thylakoids.

The fluorescence decay curves from all detection wavelength and quinone concentrations were fitted simultaneously using one of two different global model functions: a sum of four exponential decay components and a kinetic version of the excited state/radical pair equilibrium model [35].

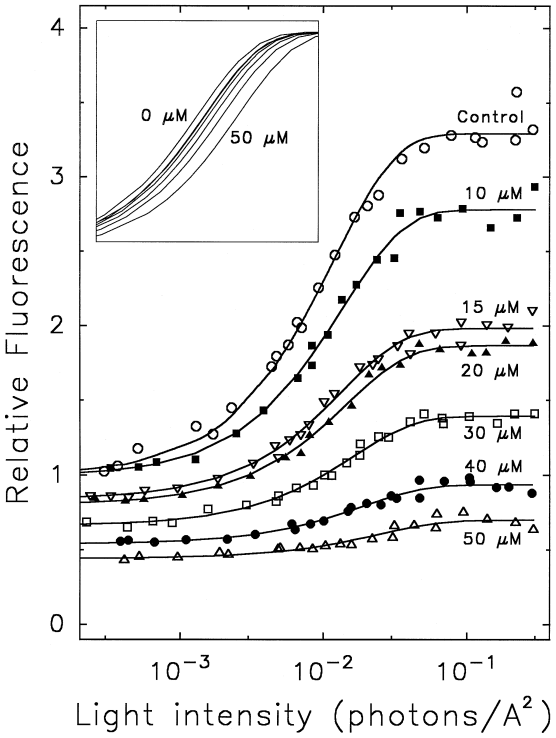

Fig. 1. Flash saturation curves of variable chlorophyll fluorescence of a 10 μM Chl thylakoid suspension in the absence and presence of various concentrations of 5-OH-NQ. See text for a full description of the pump probe technique. Fluorescence intensities are shown relative to the control in which F_0 has been set to 1.0 units. Open circles represent the control data in the absence of 5-OH-NQ. The final concentration of 5-OH-NQ used for all other experiments is shown adjacent to each data set. The lines running through the data points are the best Poisson fits to each saturation curve, see text for full details. The effective absorption cross-section (σ) of the control was 81 ± 3 Å^2. The inset shows the Poisson fits normalized to their own variable fluorescence (F_v) to facilitate visualization of the rightward shift of the curves, corresponding to smaller effective absorption cross-sections (σ), with increasing 5-OH-NQ concentration. The relative decreases in σ with respect to the control are summarized in Fig. 2.

3. Results and discussion

3.1. Absorbance cross-sections and steady state fluorescence parameters

Results of studies into the room temperature fluorescence flash saturation curves of 10 μM Chl thylakoid suspensions treated with 5-hydroxy-1,4-naphthoquinone (5-OH-NQ) are shown in Fig. 1. These curves were employed to determine the absorption cross-sections of PSII antenna. Typical flash saturation curves obtained using the pump-probe technique are shown with the best fit to each data set using the single-hit Poisson distribution. For each curve fluorescence arising from the probe flash increases from a minimal fluorescence yield (F_0) at low pump flash intensities (all PSII centres open) to a maximal fluorescence yield (F_{sat}) obtained with saturating pump flash intensities (all PSII centres closed). The relative

fluorescence values have been normalized by setting F_0 of the control to 1.0. Increasing concentrations of 5-OH-NQ were observed to decrease F_0 and to a greater extent, F_{sat}. For example, at a 50 μM quinone concentration, there was an 80% reduction in variable fluorescence ($F_v = F_{sat} - F_0$), while even the 10 μM addition elicited a 40% decrease. Increasing the quinone concentration decreased the variable fluorescence in each case.

The inset to Fig. 1 shows normalized fits to the flash saturation data (the relative fluorescence for each data set is equal to $(F(I) - F_0)/F_v$ where $F(I)$ is fluorescence at a particular light intensity). Normalization allows comparisons of the inflection points of the Poisson curves and hence a direct visualization of the decreasing absorbance cross-sections observed with increasing 5-OH-NQ. The effective absorbance cross-section of the control was 80 ± 3 Å^2 and at 50 μM quinone this was reduced to 43 ± 3 Å^2.

In all cases a single-component Poisson distribution gave satisfactory fits to our flash saturation data suggesting a homogeneous population of PSII. The cross-sections for all quinone concentrations are compiled in Fig. 2.

Fig. 2 also contains an independent study into the fluorescence parameters F_0 and F_m (the maximal fluorescence yield observed under multi-turnover saturating light conditions. The maximum Chl a emission yield induced by a single turnover saturating flash (F_{sat}) is lower than that observed under saturating multi-turnover light flashes (F_m). Several possible origins of this low yield have previously been suggested: oxidizing equivalents on the donor side of PSII, oxidized plastoquinone pool and/or an unidentified quencher Q_2 [21]. To obtain multi-turnover F_m values with our pump probe spectrometer, a background blue light was used to illuminate the sample during the pump probe measurement. Consistent with earlier reports [21], F_m was 25% higher in the control thylakoids than F_{sat}. Interestingly, the difference between F_m and F_{sat} disappeared in the presence of any concentration of 5-OH-NQ used (data not shown). This finding supports the proposal [33] that oxidized quenchers, possibly the endogenous PQ pool or an unidentified quencher termed Q_2, may be a source of low fluorescence yield induced by single turnover flashes.

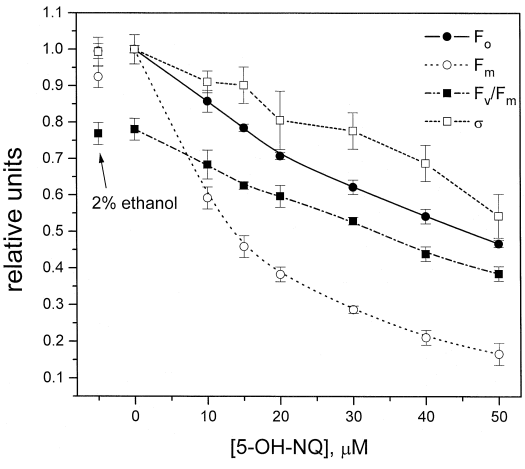

Fig. 2. Effects of exogenous quinones on relative fluorescence parameters and relative absorption cross-sections of PSII for thylakoid suspension. Errors, in brackets, are ±standard deviation.

As shown in Fig. 2, all parameters: F_0, F_m, F_v/F_m, and σ decrease with increasing quinone concentration. The F_m of the thylakoids decreases much faster than F_v/F_m, and σ. The decrease in σ appears to correlate best with F_0, but is also close to that of F_v/F_m, the quantum yield of photochemistry.

Models of antenna based qN predict a decrease in σ, indicating that the probability of an incident photon to induce photochemistry at the PSII reaction centre has been decreased. Quenching arising in the reaction centre that occurs after the single turnover pump flash would not be predicted to affect the cross-section size nor would the formation of inactive PSII quenching centres which did not generate F_v. Exciton quenching in the antenna is expected to decrease fluorescence yield at both F_0 and F_m and also σ. Qualitatively, the correlation between F_0 quenching and decrease in σ is an expected trend for classical antenna quenching, providing evidence that 5-OH-NQ acts in the antenna complex. These results support the findings of other groups that have suggested some quinones quench fluorescence in the antenna complex [21,25,29].

To quantitatively assess the quenching of excited states in PSII antenna by 5-OH-NQ requires more direct measurements of excited state dynamics. To achieve these we investigated the picosecond time resolved fluorescence emission of thylakoids in the presence of the quinone.

3.2. Time resolved fluorescence measurements

More information about the origins of fluorescence quenching by 5-OH-NQ can be obtained from studies of time-resolved fluorescence decay kinetics. We fit decay kinetics detected at five different wavelengths simultaneously by global lifetime analysis. To achieve better separation between PSI and fast PSII decay components we applied a physically reasonable constraint by assuming that the fraction of PSI emission was independent of the quinone addition. We found the decay kinetics of thylakoids with open PSII reaction centers to be modeled well with a sum of four exponential decay components at quinone concentrations in the range 0–40 μM. The corresponding decay associated spectra (DAS) are shown in Fig. 3. The fastest DAS component $\tau_1 = 40–70$ ps is red shifted in comparison with other decay components, its amplitude was independent of the 5-OH-NQ concentration (in unconstrained fits) and its lifetime slightly decreased with addition of the quencher. This component probably has a composite nature (see discussion below) with major contribution from PSI. The second and third decay components $\tau_2 = 240$ and $\tau_3 = 490$ ps have similar DAS peaking around 685 nm, suggesting an origin in PSII. The fourth component $\tau_4 = 3.6$ ns had a very small relative amplitude and was virtually independent of quinone addition. The major changes in decay components observed upon quinone addition were the concomitant decrease in lifetime of the second component and decrease in amplitude and lifetime of the third component.

Previous studies on the fluorescence decay kinetics of pea thylakoids at F_0 and F_m showed that in general two PSII forms (PSII α and PSII β) contribute to the observed kinetics. However, it was possible to resolve these forms only using a combined analysis of decay kinetics measured both at F_0 and F_m. When analysed separately, fluorescence decay kinetics at F_0 were well described assuming a homogeneous PSII characterized by a biexponential decay with lifetimes of 290 ps and 630 ps. Three additional components (18 ps, 100 ps and 1.9 ns) were resolved [36]. In that study the fastest decay component was assigned to exciton equilibration in antenna complexes, the second component was suggested to represent PSI with some contribution from PSII β, while the third was attributed to a very minor fraction of PSII that contained closed reaction centers. Lifetimes of PSII reported by these authors are reasonably close to the values of corresponding components (240 ps and 490 ps) found in the absence of quinone in the present study. We did not resolve the fastest decay component, corresponding to the 18 ps decay observed previously. This result may be related to the relatively long excitation pulses (60 ps FWHM) used in our experiments. Therefore, the 70 ps lifetime component obtained from analysis of our data represent PSI with some possible contributions from exciton equilibration, and/or PSII β. As might be expected, the PSI component was less affected by the exogenous quencher, as indicated by its smaller relative decrease in magnitude. Efficiency of trapping helps to distinguish PSII from PSI antenna.

The assumption made in previous studies [36] that the longest (about 3 ns) decay component originates from closed PSII centers predicts a very pronounced quenching of this component by 5-OH-NQ. This is because the quinone quenches F_m much more efficiently than F_0 (see Fig. 2). In direct conflict with this assignment we found that the longest decay component was not greatly affected by 5-OH-NQ. Alternatively the long component found in the preparations used in this study can be assigned to a minor fraction of Chl molecules, which are functionally not connected to any of the reaction centers. Observation that 3.6 ns component peaks below 680 nm (in contrast to the 1.9 ns component in [36]) supports this conclusion. It has previously been suggested that quinone binding sites are localized in close vicinity to the reaction centers of PSII [37,38]. The observation that disconnected antenna complexes do not exhibit a pronounced quenching by quinones in the range of concentrations up to 50 μM 5-OH-NQ supports this idea.

3.3. Kinetic modeling of fluorescence decays and absorbance cross-sections

To further analyse the nature of fluorescence quenching by 5-OH-NQ we made an attempt to apply the exciton/radical pair equilibrium model [35] to explain both the excited state dynamics and effective absorption cross-sections of PSII in the presence of exogenous oxidized quinone. In this procedure the

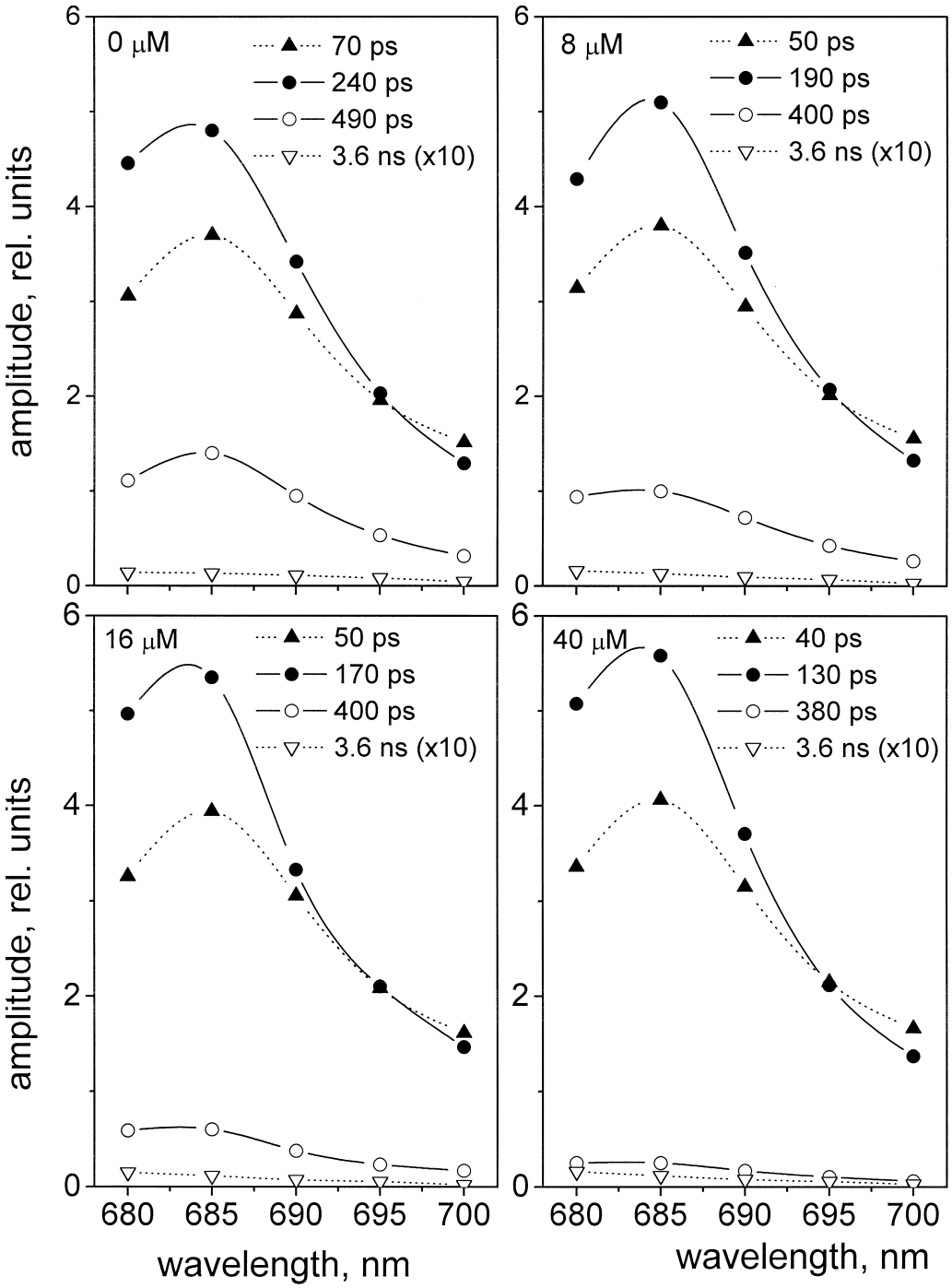

Fig. 3. Decay-associated spectra of spinach thylakoids at F_0 as calculated from the amplitudes of the four components used in the global lifetime analysis of the fluorescence decay kinetics. The amplitude of the 3 ns component has been multiplied by 10. The amount of added 5-OH-NQ for each experiment is shown at the top of each panel.

exciton/radical pair equilibrium model was fitted to the set of decay kinetics. A simplified kinetic pattern of the exciton/radical pair equilibrium model used is shown in Fig. 4. According to this model PSII is characterized by a set of rate constants (k_A, $k_Q(Q)$, k_{PC}, k_{ST}) and by an amplitude factor, which is

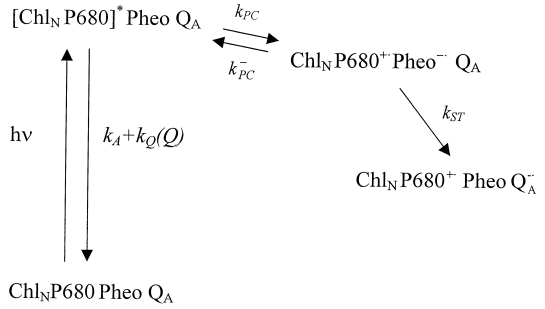

Fig. 4. Exciton/radical pair equilibrium model for primary processes in PSII [35]. [Chl$_N$P680]* symbolizes the exciton equilibration among N antenna Chl molecules and P680. The rate constants describe excitation decay from the antenna in the absence of exogenous quencher (k_A), quenching of excitations in equilibrated antenna by quinone ($k_Q(Q)$), the primary charge separation (k_{PC}), its reversal ($k_{\bar{P}C}$) and stabilization by rapid electron transfer from Pheo$^-$ to Q_A (k_{ST}).

proportional to the number of Chl's functionally connected to PSII. To account for the fluorescence decay components not associated with PSII (PSI and disconnected Chl) two exponential components with parameters A_i and τ_i were added to the kinetics of the model. Excitation probability flow in the model system was calculated from an analytical solution of the set of coupled differential equations. All parameters were fitted directly to the experimental decay curves using a nonlinear Levenberg–Marquardt algorithm (modified mqrmin routine from Numerical Recipes in C library). By performing kinetic modeling of the data we hoped to determine the effect of 5-OH-NQ on the set of rate constants describing relaxation processes in PSII. The key advantage of this type of analysis is that fitting is performed in space of the rate constants, which describe physical properties of the system. A specific model is fit to the whole experiment, reasonable physical constraints can be set by the linking of data sets measured at different conditions (e.g., varying quinone concentration).

In global target fitting procedure we used the same constraint on PSI as for the global lifetime analysis and made one more physically reasonable assumption which requires that quinone quenching may result in alteration of k_A and k_{ST} while k_{PC} and its reversal were unaffected. In this approach all decay kinetics, collected at four quinone concentrations and five wavelengths, were fit simultaneously. Note that the system of equations is characterized by the four rate constants and to solve it one of them has to be fixed. In previous studies [35,39,40] k_A was set to the value derived from the fluorescence lifetime of the isolated LHC II complex (0.2–0.3 ns^{-1}). In terms of the kinetic model the addition of quinone increases the number of equations with the same variables and thus allows solution of the system for all rate constants. The values of the rate constants obtained from this analysis are compiled in Table 1. Addition of 5-OH-NQ was found to accelerate the decay of excitation in the antenna drastically. The corresponding rate constant $k_A + k_Q(Q)$ increased from 0.3 ns^{-1} in control samples to 3.23 ns^{-1} in samples with 40 μM of 5-OH-NQ.

As discussed above, PSII was previously found to be kinetically heterogeneous at F_m [36]. Authors of the latter study attempted to resolve two pools within PSII at F_0 using a PSII α/PSII β ratio derived from fitting of the F_m data. Analysis of that data performed in terms of a heterogeneous exciton/radical pair

Table 1
Results from the global analysis of the fluorescence decay kinetics of spinach chloroplasts at increasing concentrations of 5-OH-NQ. χ^2 values generated for fits ranged between 0.96 and 1.23. The relative amplitudes at 685 nm are given in parentheses. The data presented are the means of three independent experiments. The uncertainty in $k_{\bar{P}C}$ and k_{ST} is about 25% and 15% correspondingly. The uncertainty in lifetimes, amplitudes and other rate constants is approximately 10%

[5-OH-NQ]	Lifetimes (ns)			Rate constants (ns^{-1})			
	PSI	PSII	Disconnected	k_{PC}	$k_{\bar{P}C}$	k_{ST}	$k_A + k_Q(Q)$
0 μM	0.07 (37%)	0.24, 0.49 (48%, 14%)	3600 (1.4%)	3.3	0.21	2.13	0.3
4 μM	0.05 (38%)	0.22, 0.44 (49%, 12%)	3600 (1.4%)	3.3	0.21	2.06	0.53
8 μM	0.05 (38%)	0.19, 0.40 (51%, 10%)	3600 (1.6%)	3.3	0.21	2.13	0.86
16 μM	0.05 (39%)	0.17, 0.40 (53%, 6%)	3600 (1.5%)	3.3	0.21	2.08	1.22
28 μM	0.05 (39%)	0.14, 0.39 (55%, 3.7%)	3600 (1.7%)	3.3	0.21	2.13	2.38
40 μM	0.04 (40%)	0.13, 0.38 (55%, 2.5%)	3600 (1.6%)	3.3	0.21	2.04	3.23

equilibrium model showed that at F_0 both PSII α and PSII β are characterized by very similar sets of rate constants [35]. Our assumption of a homogeneous PSII at F_0 is therefore well justified. The values found for the rate constants $k_{PC} = 3.3\ ns^{-1}$, $k_{PC}^{-} = 0.21\ ns^{-1}$ and $k_{ST} = 2.1\ ns^{-1}$ are very close to the corresponding values reported for pea thylakoids ($2.7\ ns^{-1}$, $0.34\ ns^{-1}$ and $2.1\ ns^{-1}$) [35].

Modified Stern–Volmer analyses have been used extensively to examine quenching efficiency of quinones in photosynthetic systems [23,26,29]. In these studies the binding constant was obtained from analysis of the Chl fluorescence yield. However, in PSII, excited states of antenna Chl's are quenched even in the absence of exogenous oxidized quinone by reaction centers executing reversible photochemical reactions (charge separation, charge recombination and charge stabilization [35,41]. Therefore, thorough analysis of quenching in the antenna of PSII requires consideration of the effects induced by these reactions. The rate constant for excitation decay from the antenna $(k_A + k_Q(Q))$ is directly related to quinone quenching. A global target analysis of the fluorescence decay kinetics at various quinone concentrations revealed that $(k_A + k_Q(Q))$ increases gradually with increasing quinone concentration. Stern–Volmer plots of $(k_A + k_Q(Q))$ and fluorescence yields at F_0 and F_m are presented in Fig. 5. The value of k_{SV} obtained for F_0 is of the same order of magnitude as that found by other groups [42] while the real k_{SV} derived from the exciton/radical pair equilibrium model is about an order of magnitude larger. The $(k_A + k_Q(Q))$ values obtained from the linear fit to the Stern–Volmer plot were used then to compute cross-sections at different quinone concentrations using the exciton/radical pair equilibrium model.

As discussed above, dependence of PSII absorption cross-sections on quinone concentration qualitatively corresponds to quenching in the antenna. Quantitatively the relative changes of absorption cross-sections can be derived from the exciton/radical pair equilibrium model as follows:

$$\frac{\sigma}{\sigma_Q} = \frac{\Phi}{\Phi_Q} = \frac{k_A + k_Q(Q) + k_{PC} - k_{PC}^{-}}{k_A + k_{PC} - k_{PC}^{-}} \qquad (1)$$

Where Φ and Φ_Q yield of Q_A^- without and with quencher correspondingly. The $(k_A + k_Q(Q))$ values

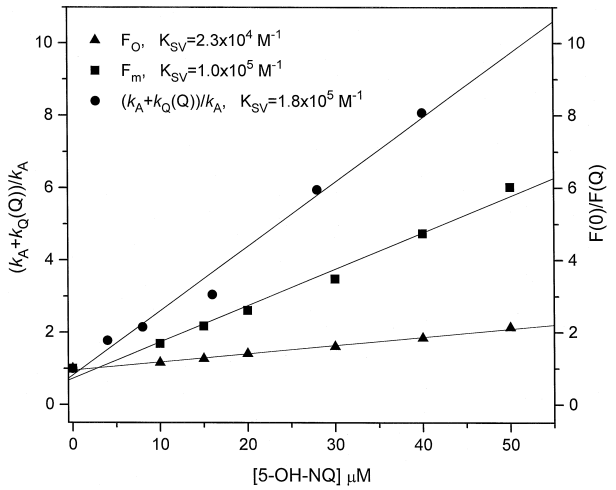

Fig. 5. Stern–Volmer analysis of fluorescence quenching by 5-OH-NQ. Quenching of the steady state fluorescence parameters F_0 and F_m ($F(0)/F(Q)$) are compared to the quenching of the rate constant for excitation decay from the antenna ($k_A + k_Q(Q))/k_A$). The Stern–Volmer constants k_{SV} derived from the slope of the curves are shown on the figure.

used to calculate cross-sections at different quinone concentrations were obtained from a linear fit to the Stern–Volmer plot (Fig. 5). Note that the relative changes of the F_0 yield follow the same law, therefore one would expect to observe an agreement between all of these parameters. The measured cross-sections, fluorescence yields and calculated cross-sections are presented in Fig. 6. The best correlation was observed between model cross-sections and F_0 yields (measured in pump-probe experiments or calculated from DAS considering all decay components). Note that F_0 obtained this way included contributions from all fluorescing pigments and, therefore, was somewhat overestimated. Consideration of only PSII DAS components resulted in somewhat lower F_0. The difference in relative changes of F_0 were found to be pronounced only at highest quinone concentration (40 μm): 0.48 (only PSII components) instead of 0.56 (all components). This corresponds to 17% overestimation of F_0. Compared with the experimental error for calculated PSII F_0 yield (15%) this difference is not significant. Surprisingly, measured cross-sections exhibit a somewhat different dependence on the concentration of quinone than it is predicted. The slope of the Stern–Volmer plot for measured cross-

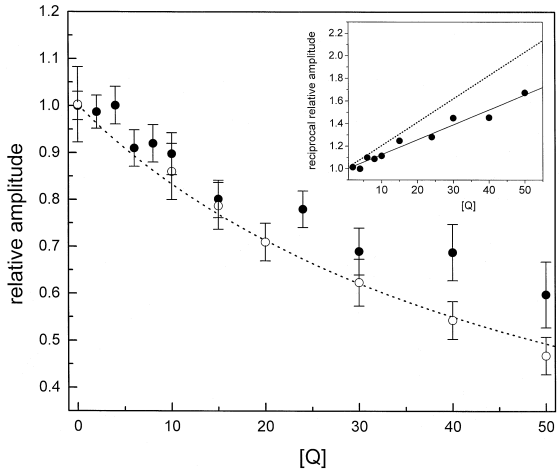

Fig. 6. The quenching of F_0 is compared to the decrease in absorbance cross-section with increasing 5-OH-NQ concentration. Open circles are normalized F_0 data from either pump probe or fluorescence decay data (sum of $\tau \times$Amplitude of all components from Fig. 2); filled circles are normalized absorbance cross-sections. The dotted line is the modeled cross-section calculated from Eq. (1) using values for k_A derived from the Stern–Volmer analysis shown in Fig. 5.

sections (inset Fig. 6) is less steep. The second trend in the data is that cross-sections appear not to decrease at the low (0–5 μM) quinone concentrations, where the steepest decrease is expected. The origin of these differences is not clear at the moment. Probably, the homogeneous exciton/radical pair equilibrium model is not good enough to describe relaxation in intact thylakoids processes owing to presence of some overlapping unresolved lifetime components. The heterogeneity with respect to a molecular functioning of two photosystems II has to be taken into account. Further experiments including simultaneous analysis of decay kinetics collected at both F_0 and F_m levels are needed to elucidate possible effects of PSII heterogeneity. This problem will be addressed in forthcoming studies.

4. Conclusions

Pump-probe and picosecond time-resolved fluorescence techniques were employed to elucidate the mechanism of non-photochemical quenching of chlorophyll fluorescence by 5-hydroxy-1,4-naphthoquinone and to characterize the experimental manifestations of that mechanism. It appears that this exogenous oxidized quinone acts in the antenna complex of photosystem II by stealing excited state energy from chlorophyll molecules. The observed decreases in F_0 and σ are tell-tale indicators of reactivity in the antenna complex. These conclusions were confirmed by analysis of the rate constants for primary processes in PSII. Depressions in F_0 and PSII absorption cross-sections, along with an increase of the rate constant for excitation decay in antenna provide ample evidence of an antenna mechanism of qE for 5-OH-NQ.

In vivo mechanisms of qN and qE that contribute to energy dissipation in higher plants are still a source of some controversy. We have demonstrated in this study that the application of a kinetic model for PSII to a combined data set of fluorescence decay kinetics and absorbance cross-section measurements can be used to quantify antenna quenching by a model antenna quencher, 5-OH-NQ. This approach is a first step towards quantifying the amount of antenna quenching contributing to qE in vivo. Used in conjunction with results from an earlier complementary report on reaction centre based quenching [21] we hope to quantitatively evaluate the contributions of antenna and reaction centre mechanisms to qE and localize the sites of qE energy dissipation in intact plant systems.

The constraints arising from the use of independent measures (fluorescence decay kinetics and absorbance cross-sections) in combination with the presence of an additional variable (quinone concentration) in our global kinetic analyses have allowed for a powerful test of the exciton/radical pair equilibration model for excited state dynamics in PSII. Our results support the general applicability of this model for PSII but indicate that a homogeneous version is insufficient to quantitatively predict the sensitivity of PSII absorbance cross-section to quinone quencher.

Acknowledgements

We would like to thank the Brock electronics and machine shops for their technical assistance, and Dr. Guy Samson for his advice on thylakoid isolations, quinones, and recrystallizations. This research was

supported by operating and equipment grants from the Natural Sciences and Engineering Research Council of Canada (NSERC) to D.B.

References

[1] G. Krause, Physiol. Plant 74 (1988) 566–574.
[2] E.-M. Aro, I. Virgin, B. Andersson, Biochim. Biophys. Acta 1143 (1993) 113–134.
[3] W. Butler, Photochem. Photobiol. 40 (1984) 513–518.
[4] E. Bracht, A. Trebst, Z. Naturforsch. 49 (1994) 439–446.
[5] D. McCormac, D. Bruce, B. Greenberg, Biochim. Biophys. Acta 1187 (1994) 301–312.
[6] G. Samson, D. Bruce, Biochim. Biophys. Acta 1232 (1995) 21–26.
[7] K. Frank, A. Trebst, Photochem. Photobiol. 61 (1995) 2–9.
[8] G. Krause, U. Behrend, FEBS Lett. 200 (1986) 298–302.
[9] P. Horton, A.V. Ruban, R.G. Walters, Plant Physiol. 106 (1994) 415–420.
[10] I. Heinze, H. Dau, H. Senger, Photochem. Photobiol. 32 (1996) 89–95.
[11] B. Demmig-Adams, W.W. Adams, Photosynth. Res. 25 (1990) 187–197.
[12] A. Crofts, C. Yerkes, FEBS Lett. 352 (1994) 265–270.
[13] A.M. Gilmore, T.L. Hazlett, Govindjee, Proc. Natl. Acad. Sci., USA 92 (1995) 2273–2277.
[14] H. Yamamoto, N. Mohanty, Aust. J. Plant Physiol. 22 (1995) 231–238.
[15] A.V. Ruban, D. Rees, G. Noctor, A.J. Young, P. Horton, Biochim. Biophys. Acta 1059 (1992) 355–360.
[16] C.W. Mullineaux, A.A. Pascal, P. Horton, A.R. Holzwarth, Biochim. Biophys. Acta 1141 (1993) 23–28.
[17] A.V. Ruban, P. Horton, Photosynth. Res. 40 (1994) 181–190.
[18] A. Ruban, P. Horton, B. Robert, Biochemistry 34 (1995) 2333–2337.
[19] D. Rees, P. Horton, Biochim. Biophys. Acta 1016 (1990) 219–227.
[20] A. Krieger, I. Moya, E. Weis, Biochim. Biophys. Acta 1102 (1992) 167–176.
[21] D. Bruce, G. Samson, C. Carpenter, Biochemistry 36 (1997) 749–755.
[22] L.K. Thompson, G.W. Brudwig, Biochemistry 27 (1987) 6653–6658.
[23] G. Seely, Photochem. Photobiol. 27 (1978) 639–654.
[24] D. Huppert, P.M. Rentzepis, G. Tollin, Biochim. Biophys. Acta 440 (1976) 356–364.
[25] K. Karukstis, S. Gruber, J. Fruetel, S. Boegeman, Biochim. Biophys. Acta 932 (1988) 84–90.
[26] K. Karukstis, M. Berliner, C. Jewell, K. Kuwata, Biochim. Biophys. Acta 1020 (1990) 163–168.
[27] K. Karukstis, K. Birkeland, B. Babusis, K. Kasal, C. Jewell, J. Luminescence 51 (1992) 119–128.
[28] P. Booth, B. Crystall, L. Giorgi, J. Barber, D. Klug, G. Porter, Biochim. Biophys. Acta 1016 (1990) 141–152.
[29] J. Amesz, D. Fork, Biochim. Biophys. Acta 143 (1967) 97–107.
[30] J.W. Lee, W. Zipfel, T.G. Owens, J. Luminescence 51 (1992) 79–85.
[31] J. Whitmarsh, D. Ort, Arch. Biochem. Biophys. 231 (1984) 3378–3389.
[32] R. Zeigler, K. Egle, Beitr. Biol. Pflanzen. 41 (1965) 11–37.
[33] G. Samson, D. Bruce, Biochim. Biophys. Acta 1276 (1996) 147–153.
[34] D. Mauzerall, N.L. Greenbaum, Biochim. Biophys. Acta 974 (1989) 119–140.
[35] G.H. Schatz, H. Brock, A.R. Holzwarth, Biophys. J. 54 (1988) 397–405.
[36] T.A. Roelofs, C.-H. Lee, A.R. Holzwarth, Biophys. J. 61 (1992) 1147–1163.
[37] K. Pfister, H.K. Lichtenhaler, G. Burger, H. Musso, M. Zahn, Z. Naturforsch. 36c (1981) 645–655.
[38] S. Berens, J. Scheele, W.L. Butler, D. Magde, Photochem. Photobiol. 42 (1985) 51–57.
[39] G. Zucchelli, R.C. Jennings, F.M. Garlaschi, Biochim. Biophys. Acta 1099 (1992) 163–169.
[40] G. Renger, H.-J. Eckert, A. Bergmann, J. Bernarding, B. Liu, A. Napiwotzki, F. Reifarth, H.J. Eichler, Aust. J. Plant Physiol. 22 (1995) 167–181.
[41] H. Dau, Photochem. Photobiol. 60 (N1) (1994) 1–23.
[42] K. Karukstis, S.C. Boegeman, J.A. Fruetel, S.M. Gruber, M.H. Terris, Biochim. Biophys. Acta 891 (1987) 256–264.